Available online at www.sciencedirect.com

ScienceDirect

Procedia Structural Integrity 47 (2023) 383–397

Structural Integrity Procedia

www.elsevier.com/locate/procedia

27th International Conference on Fracture and Structural Integrity (IGF27)

Quasi-static and dynamic response of cardanol bio-based epoxy resins: effect of different bio-contents

Andrea Iadarola[a]*, Pietro Di Matteo[b], Raffaele Ciardiello[a], Francesco Gazza[c], Vito Guido Lambertini[c], Valentina Brunella[b], Davide Salvatore Paolino[a]

[a]*Department of Mechanical and Aerospace Engineering, Politecnico di Torino, C.so Duca degli Abruzzi 24, Turin 10039, Italy.*
[b]*Department of Chemistry, Università degli Studi di Torino, Via Pietro Giuria 7, Turin 10125, Italy.*
[c] *Material Sustainability Engineering Department, Centro Ricerche Fiat (Stellantis), C.so Giovanni Agnelli 220, Turin 10135, Italy*

Abstract

In recent years, the European Community regulations are promoting the use of sustainable and green materials to lower the overall carbon footprint, especially in the automotive sector. The majority of structural composite materials use petrol-based epoxy matrices which are not easily recyclable, thus representing a negative impact on the environment. The most promising and ready-to-use technology to lower the carbon footprint in composite materials is the use of bio-based resins partially derived from renewable resources since this replacement is not affecting the manufacturing processes. Two commercial resins, a cardanol-based epoxy resin (27% bio-content) and an epoxy novolac resin (84% bio-content), were mixed to obtain four different resin mixtures. In particular, the higher bio-content novolac resin was mixed with the cardanol epoxy resin in different weight percentages to reach a total bio-content higher than 27%. The resins obtained by this procedure are characterized by total bio-contents of 27%, 31%, 41% and 51%, calculated on biomass used in production. Quasi-static and dynamic tensile tests have been carried out to assess the mechanical behavior of the different resins at increasing bio-contents. The strain has been acquired by using Digital Image Correlation (DIC) system to determine the failure modes with respect to the bio-content. The tests have shown that the increase of bio-content lead to lower Young's modulus and lower ultimate strengths both decreasing with a linear trend in static and dynamic conditions. The glass-transition temperatures (T_g) of each mixture have been also studied by means of Differential Scanning Calorimetry (DSC) analyses to assess the effect of the bio-content on the T_g values.

Keywords: biopolymers, bio based epoxy resin, cardanol, composites, glass transition, chemical, mechanical, quasi-static, dynamic, tensile test.

* Corresponding author.
E-mail address: andrea.iadarola@polito.it (A. Iadarola)

10.1016/j.prostr.2023.07.086

1. Introduction

In the last years, environmental and economic concerns related to petrochemical resources are growing, thus stimulating research and development of bio-based solutions. Green polymers and composites deriving from renewable resources are sustainable solutions for companies and customers due to the reduction of petroleum resources needed in production [1]. The shift to more sustainable materials in the automotive industry is also driven by European regulations [2] aiming at lowering the overall carbon footprint.

Epoxy resins have represented for a long time one of the most employed resin systems and, for this reason, various types of commercial bio-based epoxy resins have been recently developed, depending on the molecular weight, epoxy equivalent weight (EEW) and viscosity [3–7].

However, epoxy resins exhibit some critical issues, mainly associated with the toxicity of some of their precursors, which are typically derived from fossil resources. Polymers obtained from natural resources, such as carbohydrates, starch, proteins, fats, and oils, have attracted increasing interest because of their low cost and biodegradability. Among these, cashew nutshell liquid (CNSL) is considered one of the most important material due to its structural features, abundant availability, and low cost [8–11]. Cardanol is one of the main components of CNSL and it can be obtained after distillation and hydrogenation process. The Cardanol-epoxy resin exhibits low transition glass temperature (T_g) and low mechanical properties, but very interesting thermal stabilities [5–8]

Terry and Taylor [12] have selected several commercial bio-based epoxy systems and they have compared their properties with those of standard petroleum-based epoxy systems, the most promising bio-based resin that they have identified is characterized by a tensile modulus of about 3090 MPa and a tensile strength of about 68 MPa. They have also identified the possible approaches that can be adopted by the manufacturers to increase the total bio content of the epoxy resin. Generally, the highest bio-content resins can be produced with conventional curing agents and by adding the bio content using Epicerol or other bio-based precursors, such as CNSL and glycerol. Gour et al. [13, 14] have investigated the possibility to toughen an epoxy novolac resin by the addition of a cardanol bio-based epoxy novolac resin in different weight percentages. They have observed a decrement of the T_g values with an increment in cardanol-based resin content, indicating a toughening effect on the base resin. Moreover, they have observed a decrement of about 10% and 12.5% in tensile strength and elongation, respectively, by adding 30% in weight of the bio-based epoxy novolac resin. Moreover, they observed an increment in their flexibility. In a preliminary activity [15], the comparison between a petrol-based and a bio-based epoxy system has been studied and also in this case the elongation to failure was found to be larger for the bio-based resin in the range of 6.6–6.9%.

In the literature [9, 16–27], together with commercial bio-based epoxy systems, there are also many examples of bio-based resins obtained by synthetization in laboratory for research purposes that may reach very high total bio-contents. For example, Shibata et al. [19] successfully used tannic acid as a curing agent with epoxidized soybean oil, creating a fully bio-based epoxy resin with a tensile strength of about 15.3 MPa and a tensile modulus of about 460 MPa. Unnikrishnan and Thachil [9, 27] have synthetized two different cardanol bio-based epoxy systems capable to originate flexible blends when incorporated with commercial epoxy resin. According to [9, 27], the incorporation of cardanol considerably enhances the ductile nature of the epoxy resin: it decreases the tensile and compressive strengths, but it significantly increases the elongation at fracture.

The present paper aims to investigate an alternative method to increase the total bio content of a commercially available bio-based epoxy system. In particular, a very high bio-content epoxy novolac resin has been mixed with a cardanol-based epoxy resin system in different weight percentages, in order to reach a higher total bio content. The effect of the bio-content on the chemical and mechanical properties of four different resin blends has been investigated by running quasi-static and dynamic tensile tests.

2. Materials and methods

This section focuses on the description of the tested resins and the experimental activity. In Section 2.1, the properties of the bio-based epoxy systems are reported, also describing the procedure adopted to mix the two different resins together. In Section 2.2, the methodology adopted to manufacture the specimen is explained. The description of the Differential Scanning Calorimetry (DSC) analysis performed on the already cured specimen is

reported in Section 2.3. Finally, the tensile testing setup and the Digital Image Correlation (DIC) system are analyzed in Section 2.4.

2.1. Bio-based epoxy systems

Two commercially available cardanol-based epoxy resins have been selected for this study. Table 1 shows the properties of the bio-based epoxy system (Cardolite® FormuLITE™ 2502A with hardener FormuLITE™ 2401B) and of the bio-based epoxy novolac resin (Cardolite® NC-547) used in this study.

Table 1. Cardanol-based epoxy resin and hardener properties [28, 29].

	Resin FormuLITE 2502A	**Hardener FormuLITE 2401B**	**Cardolite NC-547**
Appearance	Clear liquid	Light yellow liquid	Reddish brown liquid
Color	≤ 1	≤ 8	18
Viscosity @25°C [cPs]	930	90	37700
Density @ 25°C [kg/L]	1.13	0.95	0.935
Epoxide Equivalent Weight [g/mol]	190	515	840
Bio-based Content [% wt.]	25.00%	33.00%	84.00%

The technical datasheets [28, 29] used for this purpose have been provided by the supplier (Cardolite Specialty Chemicals Europe NV, Mariakerke (Gent) Belgium). Table 2 reports the chemical and mechanical properties of the bio-based epoxy system (2502A+2401B).

Table 2. Cardanol-based epoxy system properties [28]

Epoxy Resin 2502A + 2401B	**Values**	**Test method**
Mixing ratio by weight	100:33	-
Mix Viscosity @25°C [cPs]	480	ASTM D2196
Pot life, 100g mix @ 23°C [min]	125	Internal supplier method[1]
Peak exotherm, 100g mix @ 23°C [°C]	31	ASTM 2471-99
Ultimate glass transition temperature [2] [°C]	88	ASTM 3418-99
Tensile Strength [MPa]	66	ASTM D638-10
Tensile Modulus [MPa]	2893	ASTM D638-10
Tensile Elongation at break [%]	3.4	ASTM D638-10
Bio-based Content [% wt.]	27.0%	Calculated

[1] pot life is measured when the formulation reaches a limit viscosity of 10,000 cPs starting from the reference temperature.

[2] DSC scan from 0 to 200°C at 20°C/min, 2nd run.

The cardanol-based epoxy resin 2502A is a di-glycidyl ether of bisphenol A. It contains both fossil and natural compounds, the latter derived from cardanol, a by-product of cashew nut processing. On the other hand, the cardanol-based novolac epoxy resin (NC-547) is a poly-glycidyl ether of an alkenyl phenol-formaldehyde novolac resin characterized by a very high bio-content (84% biomass). The amine hardener (2401B) is a mixture of aliphatic and cycloaliphatic amines characterized by a bio-based content of 33%. It is aimed to react with the epoxide groups of the resin to form a crosslinked network. In the present study, the resin systems have been mixed in order to obtain four different blends characterized by four different total bio-contents. In particular, the higher bio-content novolac resin (NC-547) has been mixed with the cardanol-based epoxy system (2502A+2401B with 27% biomass) in different weight percentages (before curing) in order to reach a total bio content higher than 27%. A two-step

mixing process has been performed: 2502A has been first mixed with NC-547 considering the stoichiometric values obtained by the EEW calculations for 100 g of 2502A, followed by the addition of 2401B hardener in stoichiometric amounts. Both mixing processes were carried out until the achievement of a completely homogeneous mixture. Table 3 summarizes the blends obtained by this procedure with the corresponding resulting total bio-content.

Table 3. Blends considered for this study.

Blend	Total Bio-Content
(2502A+2401B) + 0% NC-547	27%
(2502A+2401B) + 10% NC-547	31%
(2502A+2401B) + 30% NC-547	41%
(2502A+2401B) + 50% NC-547	51%

The actual total bio-content has been computed using the rule of mixture, considering the addition of 10, 30 and 50% of NC-547 over 100 g of cardanol-based epoxy system (2502A+2401B).

2.2. Specimens manufacturing

The geometry of the specimen (Fig. 1) has been selected from ASTM D638 [30].

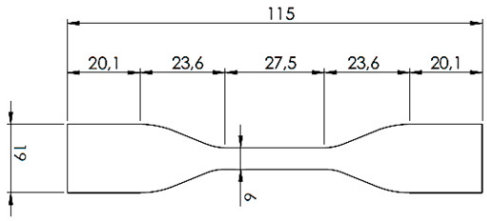

Fig. 1. Specimen geometry [30].

For what concerns the specimen production (Fig. 2), a negative mold has been first produced (Fig. 2a) by means of a 3D printer. A two-part condensation cure silicone rubber (Easy Composites CS25 Condensation Cure Silicone Rubber) has been poured into the negative mold. After curing for 24 hours at room temperature, the actual silicon mold with the specimen geometry aimed to contain the liquid resin mixture has been obtained (Fig. 2b).

a)

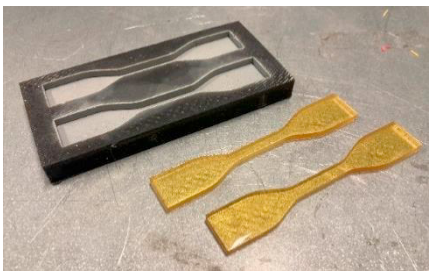

b)

c) d)

Fig. 2. Specimen production: (a) Negative mold; (b) Silicon mold; (c) Silicon mold in the curing oven with liquid resin; (d) Smoothed specimen with speckle.

Before casting the resin mixture into the silicon mold, a degassing phase (10 minutes long) has been performed to avoid the presence of bubbles and, therefore, voids in the final material. Subsequently, the silicon mold containing the resin in liquid state has been transferred in the curing oven (Fig. 2c) and the curing cycle shown in Fig. 3 has been performed (4h at room temperature + 2h at 80 °C + 2h at 120 °C).

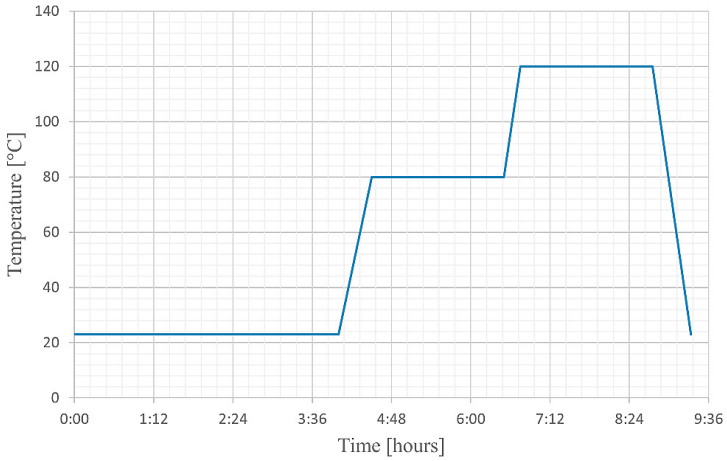

Fig. 3. Curing ramp

The curing cycle has been defined starting from the technical datasheet of the cardanol-based epoxy resin provided by the supplier and then modified considering similar works in literature [31]. After that, the cured specimen surfaces have been polished and then treated with spray paint to obtain a speckle suitable for the DIC software (Fig. 2d).

2.3. Differential Scanning Calorimetry (DSC)

DSC experiments have been performed using DSC Q200 TA Instruments. The samples have been conditioned at -40°C and then heated at a constant rate (20°C/min) from -40 to 200°C in a nitrogen (N_2) atmosphere with a constant flow rate of 50 mL/min. DSC analysis has been performed on all the cured blends to assess the effect of the bio-content on the T_g values and to verify the absence of exothermic peaks after the curing process. The T_g values have been identified using the tangent intersection method between the initial and final temperature at which the glass transition takes place.

2.4. Tensile test and DIC system

Tensile tests on the final resin mixtures have been carried out to verify the tensile properties provided by the material supplier and to assess the variability of the same properties with respect to the increase of total bio-content.

Tensile tests have been performed using an MTS Landmark (25 kN load cell) provided by the laboratories of the Material Sustainability Engineering department of Centro Ricerche Fiat (C.R.F., Stellantis group). The tensile testing machine is equipped with a DIC system (LaVision GmbH, with LaVis 10 processing software) for the acquisition of the strain data. For this purpose, a random speckle (Fig. 2d) has been sprayed on the specimen surface, to track surface displacements and calculate the material deformation. The specimens object of this study have been tensile tested in quasi-static (0.1 mm/s) and dynamic (10 mm/s and 100 mm/s) conditions. Fig. 4 shows the tensile test setup: the testing machine together with the DIC system.

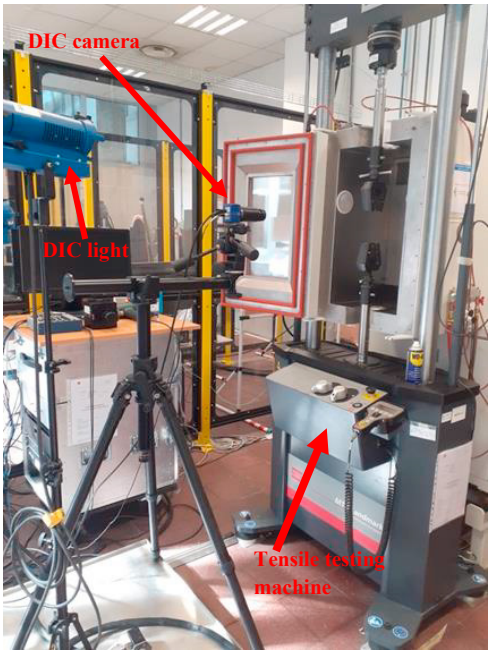

Fig. 4. Tensile testing machine and DIC configuration.

The actual width and thickness of each specimen have been measured with a digital caliper (resolution of 0.01 mm) to compute the applied stress more accurately. Three specimens have been tested for each material at each strain rate condition. The values of modulus and strength have been computed considering the mean value of the three specimens.

2.5. Optical microscopy

An optical analysis of the fracture surfaces on representative specimens has been carried out. For this purpose, a Dino-Lite AM3113T digital microscope has been used. Technical specifications are reported in Table 4.

Table 4. Technical specification of the digital microscope

Specifications	
Light/ LED type	White
Magnification	10-70x, 200x

Resolution	VGA (640x480)
Maximum frame rate	30 fps

The specimens have been placed on a support in order to keep the fracture surfaces perpendicular to the lens.

3. Results and discussion

In this section, the experimental results are commented and analyzed. In Section 3.1, the results of the DSC tests on the already cured specimens for all the analyzed materials are reported. In Section 3.2, the tensile test results on the four different bio-based mixtures are analyzed and compared, taking into account the effect of the strain rate especially for the elastic modulus and for the maximum tensile strength. Finally, in Section 3.3, representative fracture surfaces for each material are compared for the investigation of the corresponding failure modes.

3.1. Differential Scanning Calorimetry (DSC)

Before the mechanical characterization, DSC analyses have been conducted on previously crosslinked specimens, reproducing a curing cycle comparable to the real one. Fig. 5 and Table 5 show the DSC curves and the corresponding T_g values of all the cured materials analyzed in this study, respectively.

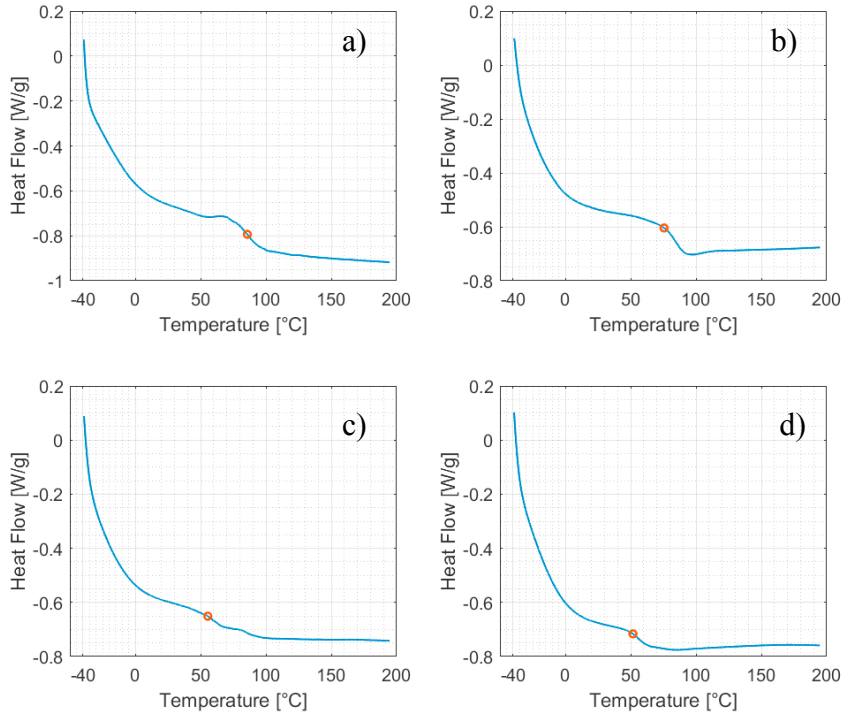

Fig. 5. DSC curves and T_g values: a) 27% total bio-content; b) 31% total bio-content; c) 41% total bio-content; d) 51% total bio-content.

The red circle on the DSC curves highlights the T_g values between the initial and final temperature at which the glass transition takes place.

Table 5. T_g values from DSC analysis at different bio-contents

Total Bio-Content	**T_g values**

27%	86°C
31%	76°C
41%	56°C
51%	52°C

The absence of peaks due to the exothermic reactions typical of the polymerization process confirms that the curing cycle adopted effectively led to the complete crosslinking of the resin mixtures. Furthermore, it is worth noting the decrement of the T_g as the bio content increases.

3.2. Tensile tests

Fig. 6 compares the stress-strain curves obtained by testing the dogbone specimens made with the investigated epoxy resin mixtures for each strain rate condition.

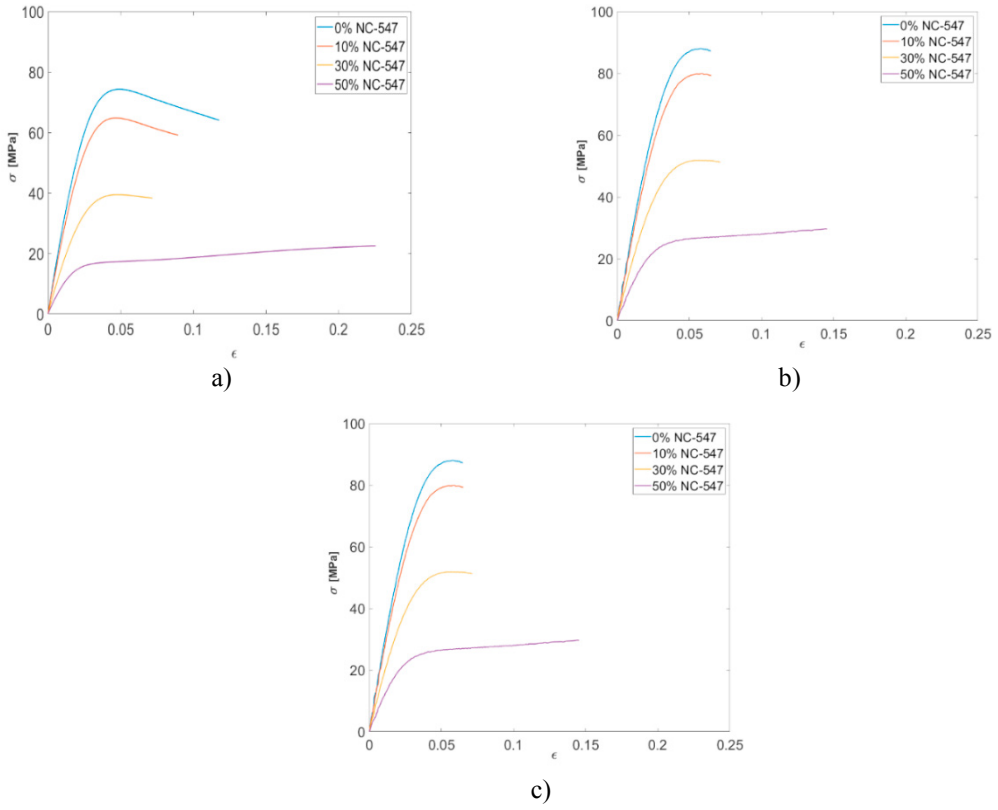

Fig. *6*. Stress-Strain curves of tensile tested materials at different strain rates to highlight the effect of the total bio-content: a) 0.1 mm/s; b) 10 mm/s; c) 100 mm/s.

These curves represent the mean curves obtained from three samples, excluding outlier specimens that prematurely failed in the linear elastic region. In both quasi-static (Fig. 6a) and dynamic (Fig. 6b, Fig. 6c) testing conditions, the curves show a reduction of strength and modulus by increasing the weight percentage addition of the epoxy novolac resin (NC-547) and so by increasing the total bio-content of the material. An increase in strength and modulus is instead observed by increasing the strain rate for all the tested materials.

Overall, it is possible to notice an increasing trend of the strain at failure by increasing the total bio-content (especially for dynamic testing conditions at 10 mm/s, Fig. 6b), even if this effect is not always visible probably due to the relevant presence of residual defects in the material that leads to a premature failure of the specimens. Fig. 6 also shows a reduction of the softening behavior by increasing both the bio-content and the strain rate. In this case, only the blend with 51% total bio-content shows a relevant increment of the strain at failure.

Fig. 7 shows the same stress-strain curves reported in Fig. 6, but in this case with the aim to highlight the effect of the strain rate for each tested blend.

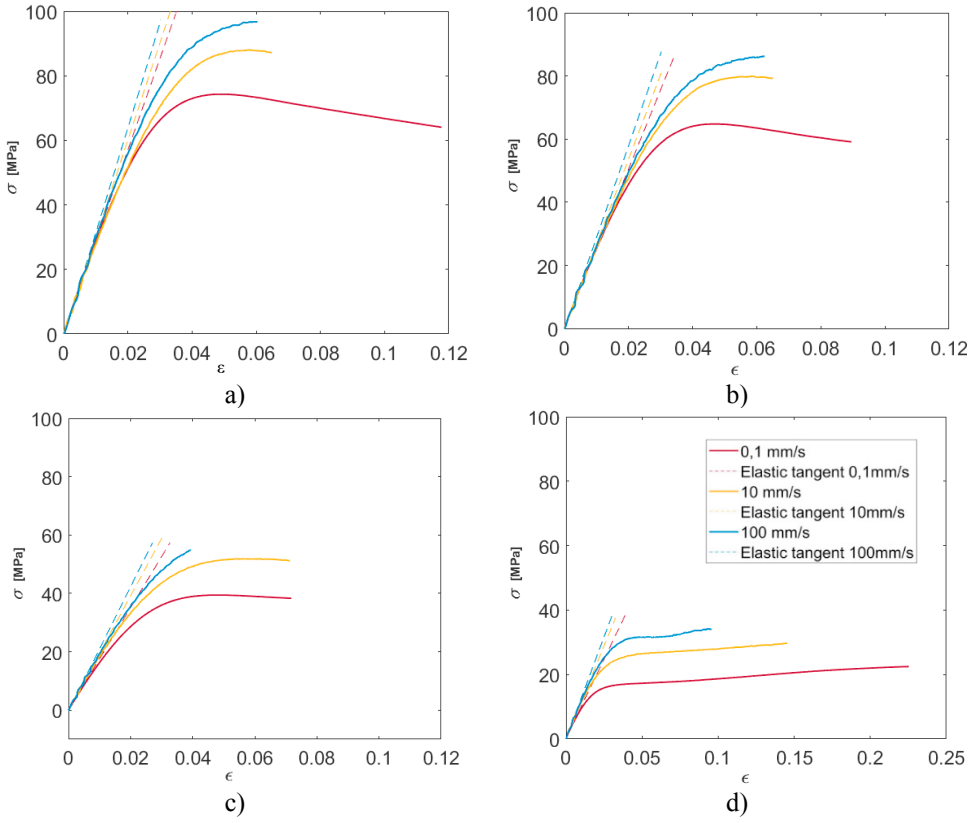

Fig. 7. Stress-Strain curves of tensile tested materials at different bio-contents to highlight the effect of the strain rate: a) 27% total bio-content; b) 31% total bio-content; c) 41% total bio-content; d) 51% total bio-content.

An increase in modulus and a reduction in maximum elongation are observed in Fig. 7 by increasing the strain rate. On the other hand, reduced strength and elastic modulus are observed in Fig. 7 by increasing the total bio content. These results are in agreement with those found in the literature [12, 14]. Moreover, the curves obtained by testing the same material at different strain rates present a good repeatability, following a similar trend by increasing the total bio-content. The mean values of the elastic modulus and the Ultimate Tensile Strength (UTS) obtained from the tensile tests are reported in Table 6 and Table 7, respectively.

Table 6. Elastic modulus mean values in quasi-static and dynamic tensile test conditions

Total Bio-Content	**Elastic modulus at 0.1 mm/s (Std. Deviation)**	**Elastic modulus at 10 mm/s (Std. Deviation)**	**Elastic modulus at 10 mm/s (Std. Deviation)**
27%	2831.5 MPa (110.00)	3014.2 MPa (130.70)	3249.6 MPa (243.00)

31%	2504.3 MPa (115.00)	2684.9 MPa (191.50)	2909.6 MPa (215.70)
41%	1752.7 MPa (145.00)	1968.1 MPa (187.00)	2131.0 MPa (29.40)
51%	981.1 MPa (82.33)	1146.5 MPa (73.95)	1264.7 MPa (111.67)

Table 6 shows the mean values of elastic modulus obtained from tensile tests and the corresponding standard deviations in order to highlight the statistical variability of the results for the three specimens tested. The values of elastic modulus are obtained with a curve fitting in the linear initial part of the curve.

Table 7. Ultimate Tensile Strength (UTS) mean values in quasi-static and dynamic tensile test conditions

Total Bio-Content	**UTS at 0.1 mm/s (Std. Deviation)**	**UTS at 10 mm/s (Std. Deviation)**	**UTS at 100 mm/s (Std. Deviation)**
27%	74.3 MPa (0.22)	88.0 MPa (0.12)	96.7 MPa (19.57)
31%	64.8 MPa (2.00)	80.0 MPa (7.60)	86.3 MPa (9.40)
41%	39.4 MPa (1.00)	51.9 MPa (0.88)	54.8 MPa (2.31)
51%	22.5 MPa (1.44)	29.7 MPa (1.10)	34.2 MPa (2.08)

Table 7 shows the mean values of UTS obtained from tensile tests and the corresponding standard deviations in order to highlight the statistical variability of the results for the three specimens tested. Fig. 8 shows the variation of elastic modulus mean values with respect to the total bio-content of the tested materials. A linear decreasing trend is observed by increasing the total bio-content of the resin and a similar decreasing slope is obtained at different strain rates.

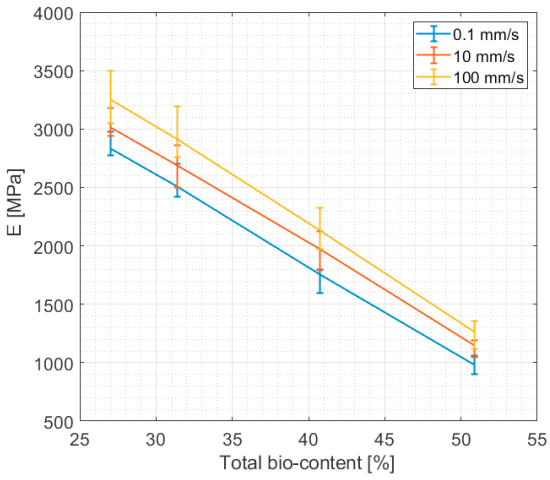

Fig. 8. Elastic modulus variation with respect to the total bio-content

The elastic modulus obtained for the un-blended material (27% total bio-content) in quasi-static testing conditions is very close to that provided by the resin supplier (Table 2), and, confirming what is shown in Fig. 6 and Fig. 7, the elastic modulus increases for higher strain rates. The elastic modulus has shown a maximum reduction in the range of 61–65% with respect to the initial value for all the strain rate conditions.

Fig. 9 shows the variation of UTS mean values with respect to the total bio-content of the tested materials.

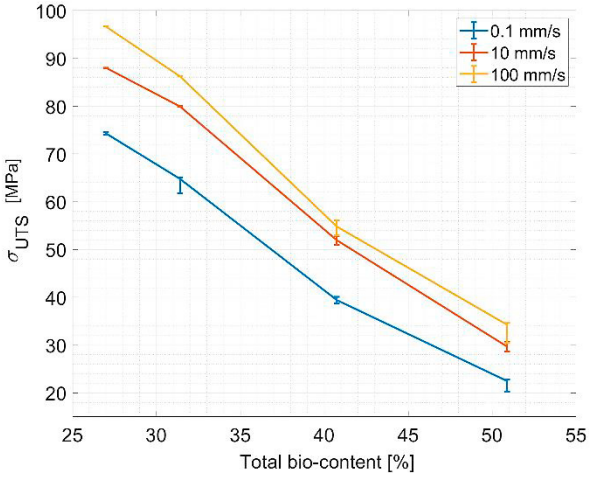

Fig. 9. Ultimate Tensile Strength variation with respect to the total bio-content

In Fig. 9, an almost linear decreasing trend is observed by increasing the total bio-content of the resin and a similar decreasing slope is obtained at different strain rates. Confirming what is shown in Fig. 6 and Fig. 7, the UTS increases for higher strain rates. For some of the tested materials, the error bars in Fig. 9 are not represented because of the exclusion of outlier values for the specimens undergoing premature failure in the linear elastic part, probably due to the presence of voids or defects.

3.3. Fracture surfaces and failure modes

Fig. 10 shows the fracture surfaces of representative specimens of the four tested materials with respect to the different strain rate conditions.

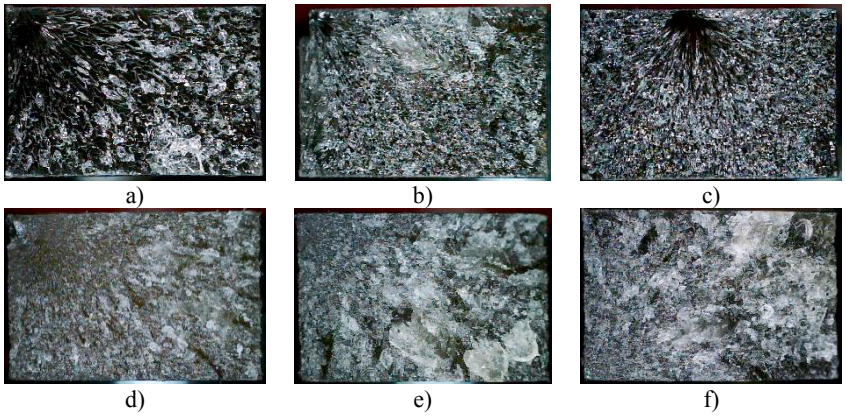

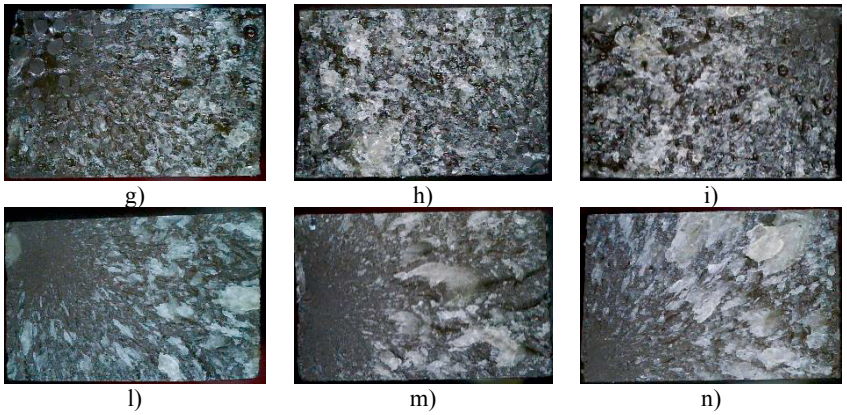

Fig. *10*. Fracture surfaces: a) 0.1 mm/s, 27% total bio-content; b) 10 mm/s, 27% total bio-content; c) 100 mm/s, 27% total bio-content; d) 0.1 mm/s, 31% total bio-content; e) 10 mm/s, 31% total bio-content; f) 100 mm/s, 31% total bio-content; g) 0.1 mm/s, 41% total bio-content; h) 10 mm/s, 41% total bio-content; i) 100 mm/s, 41% total bio-content; l) 0.1 mm/s, 51% total bio-content; m) 10 mm/s, 51% total bio-content; n) 100 mm/s, 51% total bio-content;

From an optical analysis it can be observed, in Fig. 10, a more ductile fracture by increasing the total bio-content (from top to the bottom) and a slightly more fragile fracture by increasing the strain rate (from left to right).

Most of the specimens have failed due to nucleation and propagation of a crack from a defect. Indeed, the presence of local defects can be verified with the DIC images. For example, taking into account the specimen at 27% of bio-content subjected to quasi-static tensile test (Fig. 11a and 11b), it is possible to see a concentration of strain in a specific point of the area of interest of the specimen where the crack originates.

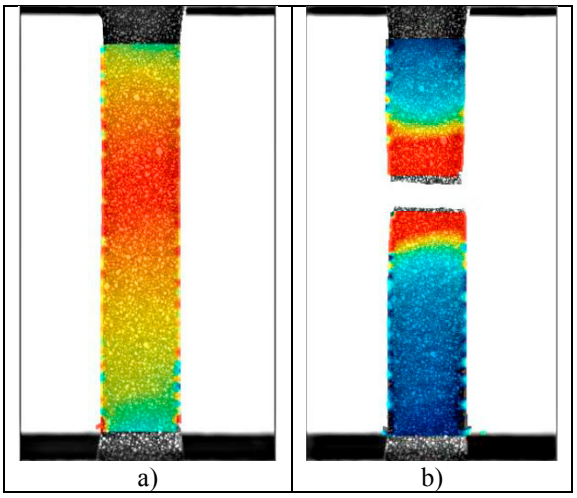

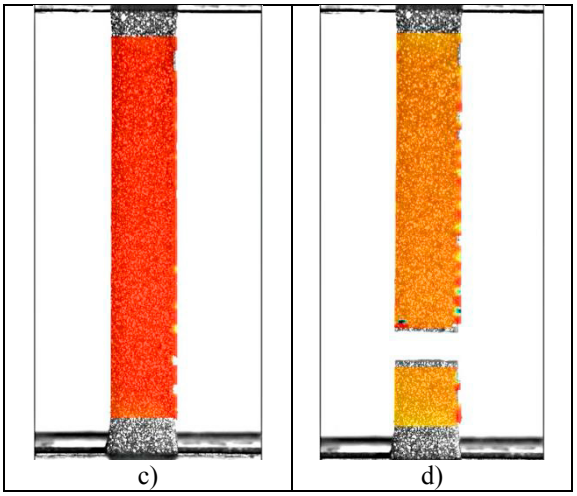

Fig. *11*. DIC images to highlight the strain concentration in presence of a defect: a) specimen 27% bio-content, just before failure; b) specimen 27% bio-content, failure instant; c) specimen 41% bio-content, just before failure; d) specimen 41% bio-content, failure instant.

For the specimens that exhibit a more uniform fracture surface, for example, the specimen with 41% of total bio-content subjected to quasi-static tensile test (Fig. 11c and 11d), the map of the strain results to be more uniformly distributed over the area of interest.

4. Conclusions

In the present paper, the effect of strain rate and total bio-content on the tensile properties of blends obtained by commercially available cardanol-based resin was analyzed. Tensile tests on four resin mixtures characterized by different total bio-contents were carried-out considering three different strain rates. Differential Scanning Calorimetry analysis of the resin mixture were performed to assess the effect of the bio-content on the transition glass temperature (T_g) values and to verify the absence of exotherm peaks after the curing process.

A reduction of the T_g values was found by increasing the total bio-content. The decrease in T_g with an increase in NC-547 content indicated the flexibilizing effect of the cardanol-based epoxy resin. The decrease in the modulus of the resin blends also revealed an increase in overall flexibility.

The increase in the total amount of bio-content led to a linear reduction of elastic moduli and strengths, whereas an increase of moduli and strengths was observed by increasing the strain rate. The stress-strain curves obtained through tensile test exhibited a reduction of the softening behavior by increasing both bio-content and strain rates, with good repeatability among the tests. The micrographs of the fracture surfaces showed no phase separation indicating good compatibility between the cardanol-based epoxy resin and the epoxy novolac resin.

In conclusion, the analyses proved that the resins with the lowest bio content have comparable properties with petrol-based epoxy resins, commonly used for structural applications. Therefore, the replacement of petrol-based epoxy resins with bio-based ones would permit a significant reduction of the environmental impact. However, manufacturing fully bio-based resin systems is a challenge that should be faced in the next future to extend their applicability in the automotive field.

References

[1] G. Koronis, A. Silva, and M. Fontul, "Green composites: A review of adequate materials for automotive applications," *Compos B Eng*, vol. 44, no. 1, pp. 120–127, 2013, doi: 10.1016/j.compositesb.2012.07.004.

[2] European Commission, *Regulation (EU) 2019/631 of the European parliament and of the council of 17 April 2019 setting CO2 emission performance standards for new passenger cars and for new light commercial vehicles, and repealing Regulations (EC) No 443/2009 and (EU) No 510/2011*. Bruxelles, 2021.

[3] S. Kumar, S. Krishnan, S. Mohanty, and S. K. Nayak, "Synthesis and characterization of petroleum and biobased epoxy resins: a review," *Polymer International*, vol. 67, no. 7. John Wiley and Sons Ltd, pp. 815–839, Jul. 01, 2018. doi: 10.1002/pi.5575.

[4] A. S. Mora, M. Decostanzi, G. David, and S. Caillol, "Cardanol-Based Epoxy Monomers for High Thermal Properties Thermosets," *European Journal of Lipid Science and Technology*, vol. 121, no. 8, Aug. 2019, doi: 10.1002/ejlt.201800421.

[5] F. L. Jin, X. Li, and S. J. Park, "Synthesis and application of epoxy resins: A review," *Journal of Industrial and Engineering Chemistry*, vol. 29. Korean Society of Industrial Engineering Chemistry, pp. 1–11, Sep. 25, 2015. doi: 10.1016/j.jiec.2015.03.026.

[6] C. S. Wang and C. H. Lin, "Synthesis and properties of phosphorus containing advanced epoxy resins," *J Appl Polym Sci*, vol. 75, no. 3, pp. 429–436, Jan. 2000, doi: 10.1002/(SICI)1097-4628(20000118)75:3<429::AID-APP13>3.0.CO;2-U.

[7] N. Pal, D. Srivastava, and J. S. P. Rai, "Studies on the effect of epoxide equivalent weight of epoxy resins on thermal, mechanical, and chemical characteristics of vinyl ester resins," *J Appl Polym Sci*, vol. 117, no. 4, pp. 2406–2412, Aug. 2010, doi: 10.1002/app.32105.

[8] S. Caillol, "Cardanol: A promising building block for biobased polymers and additives," *Current Opinion in Green and Sustainable Chemistry*, vol. 14. Elsevier B.V., pp. 26–32, Dec. 01, 2018. doi: 10.1016/j.cogsc.2018.05.002.

[9] K. P. Unnikrishnan and E. T. Thachil, "Synthesis and characterization of cardanol-based epoxy systems," *Des Monomers Polym*, vol. 11, no. 6, pp. 593–607, Oct. 2008, doi: 10.1163/156855508X363870.

[10] P. Campaner, D. D'Amico, L. Longo, C. Stifani, and A. Tarzia, "Cardanol-based novolac resins as curing agents of epoxy resins," *J Appl Polym Sci*, vol. 114, no. 6, pp. 3585–3591, Dec. 2009, doi: 10.1002/app.30979.

[11] F. Jaillet, E. Darroman, A. Ratsimihety, R. Auvergne, B. Boutevin, and S. Caillol, "New biobased epoxy materials from cardanol," *European Journal of Lipid Science and Technology*, vol. 116, no. 1, pp. 63–73, 2014, doi: 10.1002/ejlt.201300193.

[12] J. S. Terry and A. C. Taylor, "The properties and suitability of commercial bio-based epoxies for use in fiber-reinforced composites," *J Appl Polym Sci*, vol. 138, no. 20, May 2021, doi: 10.1002/app.50417.

[13] R. S. Gour, K. G. Raut, and M. V. Badiger, "Flexible epoxy novolac coatings: Use of cardanol-based flexibilizers," *J Appl Polym Sci*, vol. 134, no. 23, Jun. 2017, doi: 10.1002/app.44920.

[14] R. S. Gour, V. V. Kodgire, and M. V. Badiger, "Toughening of epoxy novolac resin using cardanol based flexibilizers," *J Appl Polym Sci*, vol. 133, no. 16, Apr. 2016, doi: 10.1002/app.43318.

[15] C. Boursier Niutta, R. Ciardiello, A. Tridello, and D. S. Paolino, "Epoxy and Bio-Based Epoxy Carbon Fiber Twill Composites: Comparison of the Quasi-Static Properties," *Materials*, vol. 16, no. 4, Feb. 2023, doi: 10.3390/ma16041601.

[16] E. A. Baroncini, S. Kumar Yadav, G. R. Palmese, and J. F. Stanzione, "Recent advances in bio-based epoxy resins and bio-based epoxy curing agents," *Journal of Applied Polymer Science*, vol. 133, no. 45. John Wiley and Sons Inc., Dec. 05, 2016. doi: 10.1002/app.44103.

[17] N. Reinhardt, J. M. Breitsameter, K. Drechsler, and B. Rieger, "Fully Bio-Based Epoxy Thermoset Based on Epoxidized Linseed Oil and Tannic Acid," *Macromol Mater Eng*, vol. 307, no. 12, p. 2200455, Dec. 2022, doi: 10.1002/mame.202200455.

[18] M. Schwaiger and K. Resch-Fauster, "Mechanical flexible epoxy resins with 100% bio-based carbon content based on epoxidized vegetable oils," *J Appl Polym Sci*, vol. 139, no. 48, Dec. 2022, doi: 10.1002/app.53233.

[19] M. Shibata, N. Teramoto, and K. Makino, "Preparation and properties of biocomposites composed of epoxidized soybean oil, tannic acid, and microfibrillated cellulose," *J Appl Polym Sci*, vol. 120, no. 1, pp. 273–278, Apr. 2011, doi: 10.1002/app.33082.

[20] C. Lorenzini, D. L. Versace, E. Renard, and V. Langlois, "Renewable epoxy networks by photoinitiated copolymerization of poly(3-hydroxyalkanoate)s and isosorbide derivatives," *React Funct Polym*, vol. 93, pp. 95–100, Jun. 2015, doi: 10.1016/j.reactfunctpolym.2015.06.007.

[21] H. Nabipour, H. Niu, X. Wang, S. Batool, and Y. Hu, "Fully bio-based epoxy resin derived from vanillin with flame retardancy and degradability," *React Funct Polym*, vol. 168, Nov. 2021, doi: 10.1016/j.reactfunctpolym.2021.105034.

[22] N. Mattar *et al.*, "Multiscale Characterization of Creep and Fatigue Crack Propagation Resistance of Fully Bio-Based Epoxy-Amine Resins," *ACS Appl Polym Mater*, vol. 3, no. 10, pp. 5134–5144, Oct. 2021, doi: 10.1021/acsapm.1c00894.

[23] M. Qi, Y. J. Xu, W. H. Rao, X. Luo, L. Chen, and Y. Z. Wang, "Epoxidized soybean oil cured with tannic acid for fully bio-based epoxy resin," *RSC Adv*, vol. 8, no. 47, pp. 26948–26958, 2018, doi: 10.1039/c8ra03874k.

[24] C. Asada, S. Basnet, M. Otsuka, C. Sasaki, and Y. Nakamura, "Epoxy resin synthesis using low molecular weight lignin separated from various lignocellulosic materials," *Int J Biol Macromol*, vol. 74, pp. 413–419, Mar. 2015, doi: 10.1016/j.ijbiomac.2014.12.039.

[25] F. Hu, S. K. Yadav, J. J. La Scala, J. M. Sadler, and G. R. Palmese, "Preparation and Characterization of Fully Furan-Based Renewable Thermosetting Epoxy-Amine Systems," *Macromol Chem Phys*, vol. 216, no. 13, pp. 1441–1446, Jul. 2015, doi: 10.1002/macp.201500142.

[26] A. Todorovic, Y. Blößl, G. Oreski, and K. Resch-Fauster, "High-performance composite with 100% bio-based carbon content produced from epoxidized linseed oil, citric acid and flax fiber reinforcement," *Compos Part A Appl Sci Manuf*, vol. 152, Jan. 2022, doi: 10.1016/j.compositesa.2021.106666.

[27] K. P. Unnikrishnan and E. T. Thachil, "The modification of commercial epoxy resin using cardanol - Formaldehyde copolymers," *International Journal of Polymeric Materials and Polymeric Biomaterials*, vol. 55, no. 5, pp. 323–338, May 2006, doi: 10.1080/009140390945178.

[28] Cardolite Corporation, "Cardolite FormuLITE 2502A + 2401B Technical Datasheet," Newark, NJ 07105, United States of America, Aug. 2017.

[29] Cardolite Corporation, "Cardolite NC-547 Technical Datasheet," May 2014.

[30] ASTM D638-14, *Standard Test Method for Tensile Properties of Plastics*. ASTM International, 2014. doi: 10.1520/D0638-14.

[31] M. Mu and A. Vaughan, "Dielectric behaviours of bio-derived epoxy resins from cashew nutshell liquid," *High Voltage*, vol. 6, no. 2, pp. 255–263, Apr. 2021, doi: 10.1049/hve2.12057.